A theoretical study of blue phosphorene nanoribbons based on first-principles calculations

Jiafeng Xie, M. S. Si, D. Z. Yang, Z. Y. Zhang, and D. S. Xue

A theoretical study of blue phosphorene nanoribbons based on first-principles calculations

Jiafeng Xie, M. S. Si,[a)] D. Z. Yang, Z. Y. Zhang, and D. S. Xue
Key Laboratory for Magnetism and Magnetic Materials of the Ministry of Education, Lanzhou University, Lanzhou 730000, China

Based on first-principles calculations, we present a quantum confinement mechanism for the band gaps of blue phosphorene nanoribbons (BPNRs) as a function of their widths. The BPNRs considered have either armchair or zigzag shaped edges on both sides with hydrogen saturation. Both the two types of nanoribbons are shown to be indirect semiconductors. An enhanced energy gap of around 1 eV can be realized when the ribbon's width decreases to ~10 Å. The underlying physics is ascribed to the quantum confinement effect. More importantly, the parameters to describe quantum confinement are obtained by fitting the calculated band gaps with respect to their widths. The results show that the quantum confinement in armchair nanoribbons is stronger than that in zigzag ones. This study provides an efficient approach to tune the band gap in BPNRs. © 2014 AIP Publishing LLC. [http://dx.doi.org/10.1063/1.4893589]

I. INTRODUCTION

Since the successful preparation[1–3] of monolayer graphite, i.e., graphene, significant efforts have been invested to understand its electronic, mechanical, thermal, and other properties.[2,4–9] One most enticing among them is the high mobility of carrier which is confined within the two-dimensional (2D) surface.[10] This makes graphene a good candidate in semiconducting and optoelectronic devices. However, it lacks a natural band gap, reducing these practical applications. The electronic band gap is an intrinsic property of semiconductors that determines the electronic transport and governs the operation of electronic devices. To this end, many other 2D materials are explored theoretically and experimentally.[11–16] A search for an intrinsic band gap is prerequisite to allow the efficient control of carriers by external field.

Unlike graphene, black phosphorus in its bulk phase is an intrinsic semiconductor with a energy gap of around 0.19 eV.[17] In theory, it can be isolated to single layer as the weak van der Waals interaction links the layers together. With this respect, two groups[18,19] independently reported that they stripped black phosphorus to few layers. It is further predicted that the energy gap can be increased to be ~0.8 eV (Ref. 19) or ~1.5 eV (Ref. 20) as black phosphorus decreases to one layer. At the same time, a strain of 10% can also introduce a considerable band gap of about 1 eV.[19,21] But this extraordinary strain is hard to access in experiment. It is a pity that these gap values are still smaller than the ideal value of ~2 eV, which directly responds to visible light.

If we change the crystal structure of black phosphorene a little, the change is dramatic. This is the case of single-layer blue phosphorus (blue phosphorene), which is theoretically predicted through using *ab initio* method.[22] It possesses an band gap of 2 eV and thus has a great potential for practical applications. Thus, it is helpful to study its electronic properties thoroughly to extend their use in semiconducting and optoelectronic devices. Experimentally, phosphorene has been produced by exfoliating its bulk, which limits its size. Nano-structured productions are common. In particular, if the monolayer is further cut into nanoribbons, an increase of band gap would be expected only considering the quantum confinement effect.[23] So far, the study of blue phosphorene nanoribbons (BPNRs) is still missing. Therefore, at present a theoretical study is timely.

In this work, we show that BPNRs with hydrogen passivated armchair or zigzag shaped edges have band gaps. The results show that the band gap increases as the decrease of nanoribbon's width, which stems from the quantum confinement effect. By fitting the calculated gaps with respect to their widths, the parameters to describe the quantum confinement are extracted. In addition, the quantum confinement effect in armchair BPNRs is more pronounced than that in zigzag BPNRs. For the case of armchair BPNRs, the quantum confinement mainly dominates the conduction band minimum (CBM). In contrast, the quantum confinement only affects the valence band maximum (VBM) for zigzag BPNRs.

The rest of this paper is arranged as follows. In Sec. II, we briefly describe the method used in this work. Results and discussion are represented in Sec. III. Finally, we conclude our work in Sec. IV.

II. METHOD

Our first-principles calculations are performed through using the SIESTA code within the framework of density functional theory (DFT).[24] The generalized gradient approximation Perdew-Burke-Ernzerhof (PBE) exchange-correction functional[25] and the norm-conserving pseudopotentials are used. The plane wave energy cutoff is set to 210 Ry to ensure
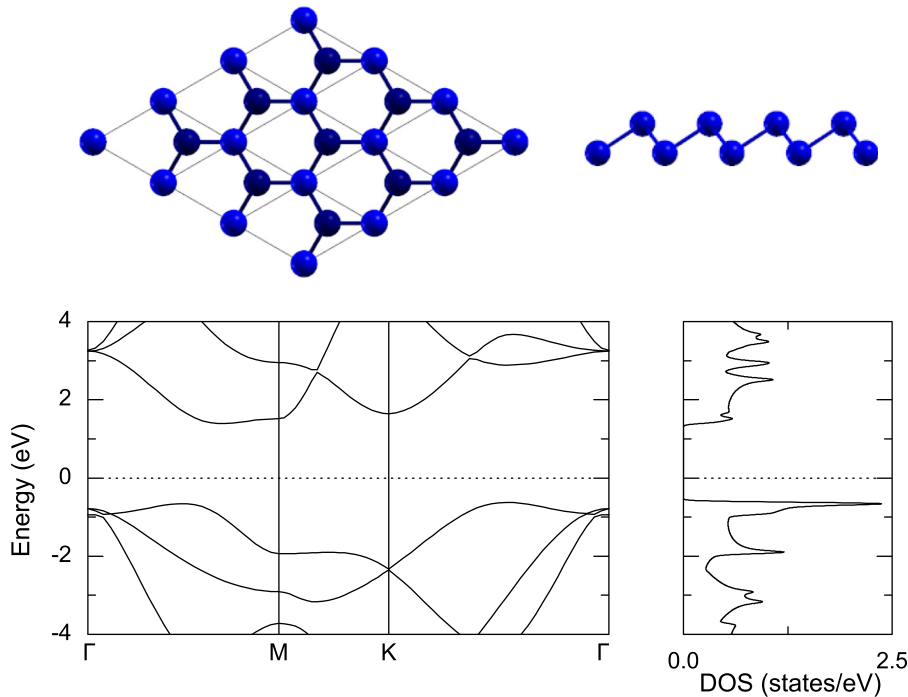
a)Email: sims@lzu.edu.cn.

FIG. 1. (a) Top (left panel) and side (right panel) views of blue phosphorene. A 3×3 supercell is taken for clarity. (b) Band structure and (c) density of states (DOS) for the blue phosphorus monolayer. The Fermi energy level is set to 0 eV.

the convergence of total energy. The reciprocal space is sampled by a fine grid of $10 \times 1 \times 1$ k-point in the Brillouin zone. The conjugate gradient algorithm is taken to fully relax the geometry until the force on each individual atom is less than 0.02 eV/Å. The optimized double-ζ orbitals including polarization orbitals are employed to describe the valence electrons. Main results are checked using VASP code and a good agreement between them is obtained.

III. RESULTS AND DISCUSSION

As a start, it is necessary to test the equilibrium configuration of blue phosphorene, as shown in Fig. 1(a). The obtained lattice constant is 3.32 Å. The P-P bond length is 2.29 Å, which is slightly larger than the P-P covalent bond length ($\sim$2.2 Å) of black phosphorus.[17] The two inequivalent P atoms are distributed in two planes with a separation of 1.26 Å (see right panel of Fig. 1(a)). All the above lattice parameters agree well with the recent theoretical results.[22] According to the band structure as shown in Fig. 1(b), the blue phosphorene is indeed a semiconductor. The highest occupied states appear at the middle region along the K-Γ line, while the lowest unoccupied states are located between the Γ and M points. It reveals an energy gap of $\sim$2 eV. It should be noticed that our band structure has a slight difference from that reported by Zhu *et al.*[22] In our case, two occupied levels are nearly degenerate at the K point below the Fermi energy level. By contrast, a gap of around 0.5 eV appears in Zhu's work.[22] At present, we cannot understand such a divergence. The DOS of blue phosphorene is displayed in Fig. 1(c), which matches the band structure well. The very localized states appear at 1 eV below the Fermi level, corresponding the highest occupied states.

Upon cutting along different directions, two types of nanoribbons of armchair and zigzag are generated, as illustrated in Fig. 2. The same denotation as graphene

nanoribbons[26] is taken for these BPNRs. Following previous convention, the armchair BPNRs are classified by the number of dimer lines (N_a) across the ribbon width. Likewise, zigzag ribbons are sorted by the number of the zigzag chains (N_z) across the ribbon width. We refer to a BPNR with N_a dimer lines as a N_a-aBNNR and a BPNR with N_z zigzag chains as a N_z-zBPNR.

It is well known that quantum confinement plays a key role when an infinite monolayer is cut into a nanoribbon. This quantum confinement has a direct effect on band gap.[27] This is also true in the case of BPNRs. Figure 3 shows the calculated band structures of the aBPNRs for three widths. Our finding is very insightful. As the width increases, the VBM remains unchanged. In contrast, the CBM moves down, which is a direct manifestation of quantum
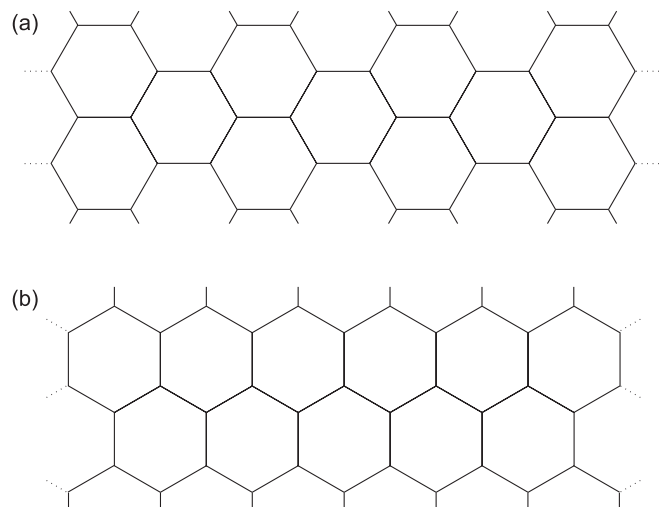

FIG. 2. (a) Armchair and (b) zigzag nanoribbons of blue phosphorene. For stabilizing the edge's state, the hydrogen saturation is taken in the realistic calculation.
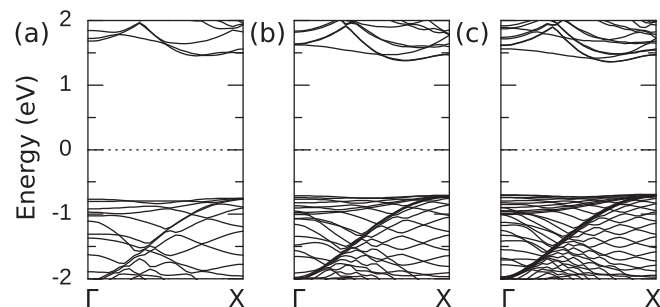
FIG. 3. Band structures of aBPNRs for three widths: (a) 11-aBPNR, (b) 19-aBPNR, and (c) 27-aBPNR. The Fermi energy level is set to 0 eV.

confinement effect in aBPNRs. In order to understand this quantum confinement better, we plot the energy gaps as a function of widths, as shown in Fig. 4. It explicitly shows that the band gap is close to 2.7 eV when the nanoribbon's width is about 10 Å. This is a big improvement compared to its infinite monolayer. As the width further increases, the energy gap decreases to be ~2 eV.

Next, we fit the theoretical gaps by $E_{gap} = E_0 + \gamma w^{-1}$ with E_0 being the band gap of blue phosphorene, w the width of nanoribons in unit of Å, and γ the quantum confinement parameter in unit of eVÅ. γ represents the strength of quantum confinement and $\gamma = 0$ corresponds to non quantum confinement. Here, we obtain $\gamma = 3.93 \pm 0.18$ eVÅ for aBPNRs. The corresponding fitted curve (solid line) is given in Fig. 4, indicating a quantitatively agreement with the calculated gaps.

To examine the underlying physics of this quantum confinement effect related to the width of aBPNRs, we plot the charge density of CBM, as shown in Fig. 5. When the width is small, the CBM locates at the middle region of aBPNR (see Fig. 5(a)). They form crescent moons, showing a strong covalent manner. As the width increases, the CBM shrinks. In other words, the edge atoms without the charge density of CBM increase. Interestingly, the charge density of CBM seems to be spherical under the large width (see Fig. 5(c)). This means its covalent character becomes weaker.

In following, we switch our focus on zBPNRs. The band structures of zBPNRs for three widths are shown in Fig. 6. They are also indirect semiconductors where the VBM is near the Γ point and the CBM is close to the X point. It is
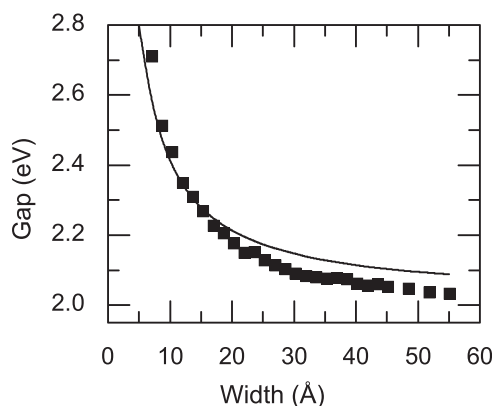

FIG. 5. The charge density of CBM for three aBPNRs: (a) 11-aBPNR, (b) 19-aBPNR, and (c) 27-aBPNR. The isovalue is set to 0.0035 e/Bohr^3. The blue and white balls represent the P and H atoms, respectively.

FIG. 6. Band structures of zBPNRs for three widths: (a) 6-zBPNR, (b) 14-zBPNR, and (c) 22-zBPNR. The Fermi energy level is set to 0 eV.

FIG. 4. The variation of energy gap as a function of width for aBPRBs. The squares are the calculated values. The solid line is the fitted curve.
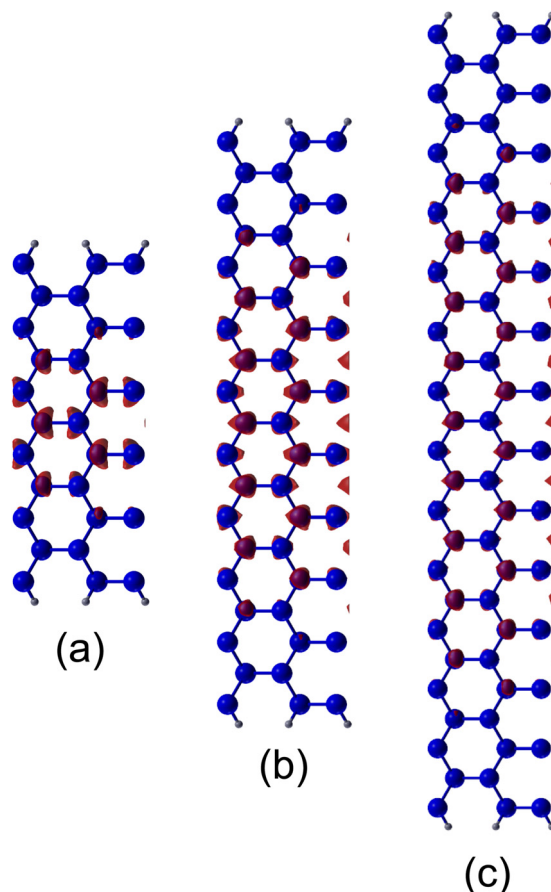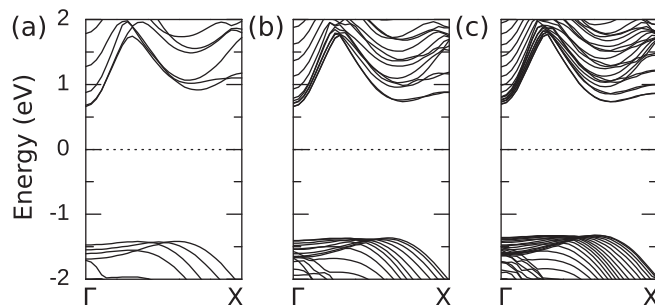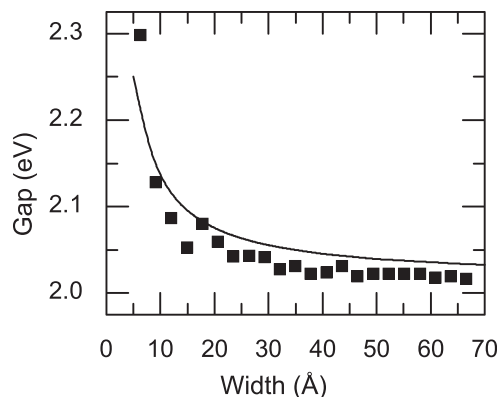

FIG. 7. The variation of energy gap as a function of width for zBPRBs. The squares are the calculated values. The solid line is the fitted curve.

also found that the widths have an effect on the band structure. In contrast, this quantum confinement only acts on the VBM near the Γ point. As the width increases, the VBM is lifted up slightly, resulting in a decrease in band gap. The detailed variation of gaps as a function of widths is displayed in Fig. 7. It explicitly shows that the band gap increases up to be $\sim$2.3 eV when the width of zBPNR is about 8 Å. If we use the above formula to fit these gaps, a good agreement is obtained (see the solid line in Fig. 7). The fitted quantum confinement parameter γ equals to 1.38 ± 0.16 eVÅ, which

is much smaller than that value $(3.93 \pm 0.18$ eVÅ) for aBPNRs. This implies that the quantum confinement in aBPNRs is stronger than that in zBPNRs.

The corresponding charge density of VBM is displayed in Fig. 8. In contrast to aBPNRs, they distribute evenly on each P atoms. As the width is small, the charge density of VBM is spherical (see Fig. 8(a)), showing a very localized feature. This makes the VBM far away from the Fermi energy level (see Fig. 6). As the width further increases, the charge density of VBM exhibit a slight polarization (see Fig. 8(c) for more details), showing a more dispersion of electronic states. As a result, the VBM will be lifted up. This is the origin of the band gap evolution with the widths of zBPNRs.

Finally, we reveal the underlying physics of scaling law for the band gap with respect to the width in BPNRs. Based on the above discussion, both aBPNRs and zBPNRs exhibit the $1/w$ scaling law, which is similar to that reported in graphene nanoribbons (GRNs). This is because GRNs are described by Dirac fermions, which obey a linear energy-momentum dispersion relation. Similarly, BPNRs are Dirac-like fermions as the bands of blue phosphorene below the Fermi level at the K point are linearly proportional to the momentum. Thus, BPNRs should follow the $1/w$ scaling law.

IV. CONCLUSION

In conclusion, we have shown that blue phosphorene nanoribbons with armchair or zigzag shaped edges all have band gaps, which decrease as the width of the system increase. The role of the quantum confinement or the width is crucial for the values for the band gaps. It provides a great potential applications in semiconducting and optoelectronic devices.
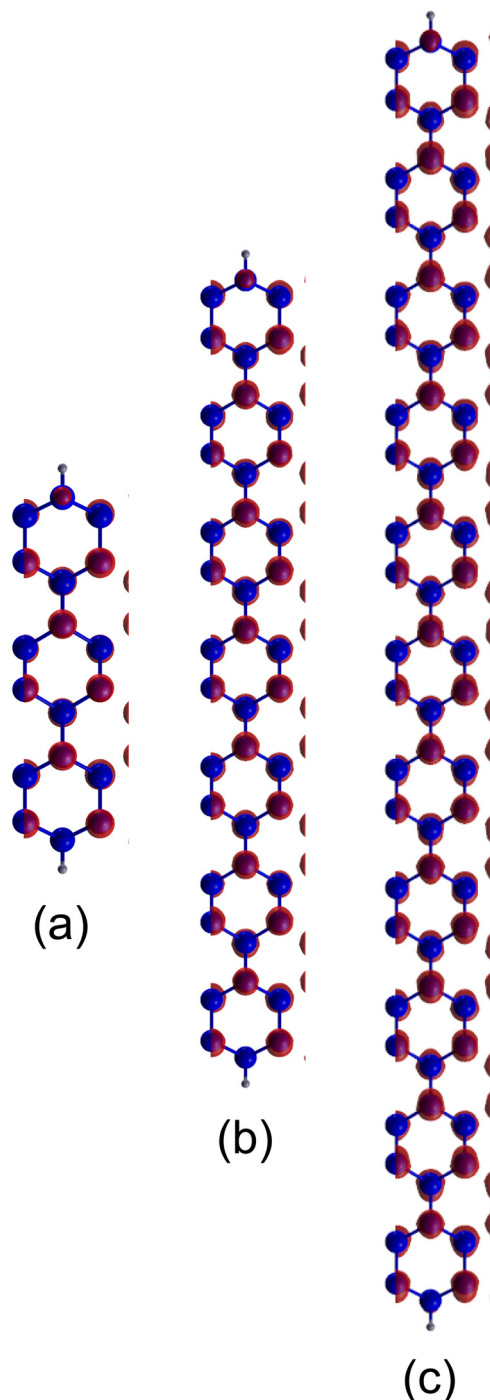
FIG. 8. The charge density of VBM for three zBPNRs: (a) 6-zBPNR, (b) 14-zBPNR, and (c) 22-zBPNR. The isovalue is set to 0.01 e/Bohr^3. The blue and white balls represent the P and H atoms, respectively.

[1]K. S. Novoselov, A. K. Geim, S. V. Morozov, D. Jiang, M. I. Katsnelson, I. V. Grigorieva, S. V. Dubonos, and A. A. Firsov, Nature (London) **438**, 197 (2005).
[2]Y. Zhang, Y.-W. Tan, H. L. Stormer, and P. Kim, Nature (London) **438**, 201 (2005).
[3]C. Berger, Z. Song, X. Li, X. Wu, N. Brown, C. Naud, D. Mayou, T. Li, J. Hass, A. N. Marchenkov, E. H. Conrad, P. N. First, and W. A. de Heer, Science **312**, 1191 (2006).
[4]A. H. Castro Neto, F. Guinea, N. M. R. Peres, K. S. Novoselov, and A. K. Geim, Rev. Mod. Phys. **81**, 109 (2009).
[5]S. Stankovich, D. A. Dikin, G. H. B. Dommett, K. M. Kohlhaas, E. J. Zimney, E. A. Stach, R. D. Piner, S. T. Nguyen, and R. S. Ruoff, Nature (London) **442**, 282 (2006).
[6]R. R. Nair, P. Blake, A. N. Grigorenko, K. S. Novoselov, T. J. Booth, T. Stauber, N. M. R. Peres, and A. K. Geim, Science **320**, 1308 (2008).
[7]A. C. Ferrari, J. C. Meyer, V. Scardaci, C. Casiraghi, M. Lazzeri, F. Mauri, S. Piscanec, D. Jiang, K. S. Novoselov, S. Roth, and A. K. Geim, Phys. Rev. Lett. **97**, 187401 (2006).
[8]A. K. Geim and K. S. Novoselov, Nature Mater. **6**, 183 (2007).
[9]P. R. Wallace, Phys. Rev. **71**, 622 (1947).
[10]E. S. Reich, Nature (London) **506**, 6 (2014).

[11]M. Corso, W. Auärter, M. Muntwiler, A. Tamai, T. Greber, and J. Osterwalder, Science **303**, 217 (2004).

[12]M. S. Si, D. Gao, D. Yang, Y. Peng, Z. Y. Zhang, D. Xue, Y. Liu, X. Deng, and G. P. Zhang, J. Chem. Phys. **140**, 204701 (2014).

[13]X. Niu, X. Mao, D. Yang, Z. Zhang, M. Si, and D. Xue, Nanoscale Res. Lett. **8**, 469 (2013).

[14]Z. Y. Zhang, M. S. Si, Y. H. Wang, X. P. Gao, D. Sung, S. Hong, and J. He, J. Chem. Phys. **140**, 1747070 (2014).

[15]P. Vogt, P. D. Padova, C. Quaresima, J. Avila, E. Frantzeskakis, M. C. Asensio, A. Resta, B. Ealet, and G. L. Lay, Phys. Rev. Lett. **108**, 155501 (2012).

[16]S. Lebégue, T. Björkman, M. Klintenberg, R. M. Nieminen, and O. Eriksson, Phys. Rev. X **3**, 031002 (2013).

[17]Y. Du, C. Ouyang, S. Shi, and M. Lei, J. Appl. Phys. **107**, 093718 (2010).

[18]H. Liu, A. T. Neal, Z. Zhu, Z. Luo, X. Xu, D. Tománek, and P. D. Ye, Nano Lett. **8**, 4033 (2014).

[19]L. Li, Y. Yu, G. J. Ye, Q. Ge, X. Ou, H. Wu, D. Feng, X. H. Chen, and Y. Zhang, Nature Nanotech. **9**, 372 (2014).

[20]J. Qiao, X. Kong, Z.-X Hu, F. Yang, and W. Ji, Nature Commun. **5**, 4475 (2014).

[21]A. S. Rodin, A. Carvalho, and A. H. Castro Neto, Phys. Rev. Lett. **112**, 176801 (2014).

[22]Z. Zhu and D. Tománek, Phys. Rev. Lett. **112**, 176802 (2014).

[23]V. Tran and L. Yang, Phys. Rev. B **89**, 245407 (2014).

[24]E. Artacho, E. Anglada, O. Diéguez, J. D. Gale, A. García, J. Junquera, R. M. Martin, P. Ordejón, J. M. Pruneda, D. Sanchez-Portal, and J. M. Soler, J. Phys.: Condens. Matter **20**, 064208 (2008).

[25]J. P. Perdew, K. Burke, and M. Ernzerhof, Phys. Rev. Lett. **77**, 3865 (1996).

[26]Y.-W. Son, M. L. Cohen, and S. G. Louie, Phys. Rev. Lett. **97**, 216803 (2006).

[27]X. N. Niu, D. Z. Yang, M. S. Si, and D. S. Xue, J. Appl. Phys. **115**, 143706 (2014).